Chemistry & Biology, Vol. 9, 455–463, April, 2002, ©2002 Elsevier Science Ltd. All rights reserved. PII S1074-5521(02)00125-4

Aminoglycosides Modified by Resistance Enzymes Display Diminished Binding to the Bacterial Ribosomal Aminoacyl-tRNA Site

Beatriz Llano-Sotelo, Eduardo F. Azucena, Jr., Lakshmi P. Kotra, Shahriar Mobashery, and Christine S. Chow[1]
Department of Chemistry
Wayne State University
Detroit, Michigan 48202

Summary

Understanding the basic principles that govern RNA binding by aminoglycosides is important for the design of new generations of antibiotics that do not suffer from the known mechanisms of drug resistance. With this goal in mind, we examined the binding of kanamycin A and four derivatives (the products of enzymic turnovers of kanamycin A by aminoglycoside-modifying enzymes) to a 27 nucleotide RNA representing the bacterial ribosomal A site. Modification of kanamycin A functional groups that have been directly implicated in the maintenance of specific interactions with RNA led to a decrease in affinity for the target RNA. Overall, the products of reactions catalyzed by aminoglycoside resistance enzymes exhibit diminished binding to the A site of bacterial 16S rRNA, which correlates well with a loss of antibacterial ability in resistant organisms that harbor these enzymes.

Introduction

The vast majority of known antibiotics inhibit the protein biosynthetic machinery by binding to the bacterial ribosome [1]. Therefore, the bacterial ribosome is a validated and important target for anti-infectives. The bacterial ribosome has a number of drug binding sites, of which the aminoacyl-tRNA site ("A site") on 16S rRNA is an important one. A number of clinically useful antibiotics, such as aminoglycosides, are known to bind to this site. We describe herein a system for quantitative assessment of the binding of antibiotics to the A site RNA. The system is based on the use of a fluorescent reporter group attached to a target RNA construct, which is sensitive to changes in the local environment. We describe the utility of this system in the analyses of binding by several aminoglycoside antibiotics and four variants of kanamycin A that are the products of modification by various resistance enzymes for these antibiotics.

Aminoglycoside antibiotics such as kanamycin (4,6-disubstituted ring II subclass) and neomycin (4,5-disubstituted ring II subclass), which were introduced to the clinic more than five decades ago [1], interact with the small subunit ribosomal RNA (16S rRNA) at the A site [2–4]. Aminoglycosides contain a number of positively charged groups at neutral pH and a significant number of hydrogen bond donor groups that contribute to rRNA binding [5–8]. Recent chemical probing and structure studies on a model 27 nucleotide RNA representing the A site of 16S rRNA revealed the significance of a noncanonical A1408•A1493 base pair for paromomycin and gentamicin binding [6–13]. The presence of the A•A motif and an adjacent bulged adenine (A1492) are critical for drug binding, mainly through interactions of rings I and II of the aminoglycosides within the major groove of the RNA. The N1 and N3 amino groups of ring II (2-deoxystreptamine) are conserved among aminoglycosides, and hydrogen bond donors are generally found at the 2′ and 6′ positions of ring I. Alterations of these conserved or semi-conserved positions would generally be expected to have deleterious effects on the RNA binding properties and antibacterial activities of the drugs.

The emergence of antibiotic resistance has become a serious problem in the treatment of bacterial infections over the past decade [14–16]. Bacteria have acquired the ability to modify the structures of the drugs in a manner that renders them ineffective as therapeutic agents [17]. In recent years, a number of enzymes that are able to modify aminoglycosides have been identified and characterized [14]. Two of the common aminoglycoside modifications include acetylation at the semiconserved 6′ amino group of ring I and phosphorylation of the 3′ hydroxyl group of the same ring [18]. A single bifunctional enzyme with the ability to modify two positions in the aminoglycosides, either individually or doubly, has also been identified [19, 20].

We describe in this report the application and general use of a fluorescent A site rRNA model in the determination of dissociation constants and binding modes of four enzyme-modified aminoglycosides. We correlate the loss of antibacterial activities of the modified aminoglycosides with their resultant diminished binding affinities to the target rRNA. These studies not only shed light on the nature of these important interactions between aminoglycoside antibiotics and RNA, but they are also valuable tools in understanding how to retain affinity for the target bacterial rRNA in the design of structural variants that can resist the modifying enzymes.

Results and Discussion

A Model for the A Site of the Bacterial 16S Ribosomal RNA

Puglisi and coworkers determined the solution structures of a 27 nucleotide A site construct complexed with paromomycin or gentamicin [6, 7]. In both cases, the conserved N1 and N3 amino groups on ring II of the aminoglycosides make direct contacts with the rRNA fragment at residues U1495 and G1494. Additional contacts are made through the hydrogen bonding groups on rings I and III. Similar observations were made in the high-resolution crystal structures of the 30S ribosomal subunit from *Thermus thermophilus* [21] and a eubacterial ribosomal decoding-region fragment [22] complexed with paromomycin. In this study, we have exploited the

[1]Correspondence: csc@chem.wayne.edu

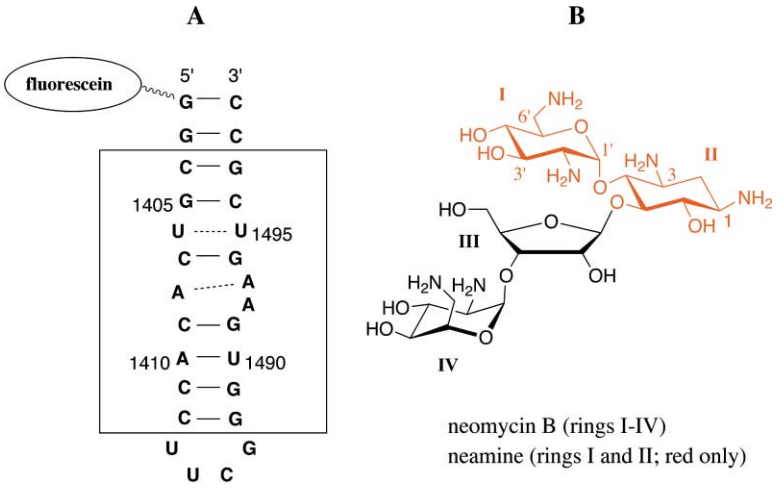

Figure 1. The 16S rRNA A Site and Neomycin Structures

(A) The sequence and secondary structure of F-AS RNA, representing the A site of *E. coli* ribosomal RNA, is shown. The boxed region shows the part of RNA representing the wild-type sequence that was used to elucidate the interactions with paromomycin and gentamicin [6, 7]. The numbering of the RNA is based on the *E. coli* 16S rRNA parent sequence.

(B) The structure of neomycin is shown with the neamine portion (rings I and II) highlighted in red.

fact that the A site RNA undergoes a local conformational change in the presence of aminoglycosides [6, 7]. Several recent studies [23–26] as well as earlier reports [27] have shown that ligand-induced conformational changes in RNA can be monitored in solution through the use of attached dye molecules. A fluorescein molecule attached to the 5′ end of the A site construct (F-AS, Figure 1A) has the ability to act as a reporter for antibiotic binding to RNA.

Binding of Neomycin to the A Site Model

Binding of the well-studied aminoglycoside neomycin (Figure 1B) to F-AS was monitored by a decrease in the fluorescence emission intensity of the attached fluorescein dye at 519 nm, as shown in Figure 2A. A binding event at low concentrations (0–50 nM) of ligand was observed. Fluorescence data were collected until saturation was reached at ≥30 nM neomycin. Fitting the curve for relative fluorescence (Fr) versus free neomycin concentration to Equation 1 (see Experimental Procedures and Figure 2B), which assumes a simple binding mode and a 1:1 complex formation, gave an apparent dissociation constant, K_d, of 5 nM (summarized in Table 1) for neomycin binding to F-AS. Similar results were obtained with 4- and 20-fold lower F-AS concentrations. Appropriate control experiments revealed that fluorescence quenching was not a result of photobleaching during the titration procedure, nor from nonspecific interactions between fluorescein and the added drug. Titrations with buffer only did not cause any changes in the fluorescence intensity of F-AS (our unpublished data). Similarly, titrations with aminoglycoside antibiotics (millimolar concentrations) did not lead to any changes in the fluorescence intensity of free fluorescein or a 5′-fluorescein-tagged GG dimer. Furthermore, fluorescence was restored upon the addition of non-fluorescein-tagged A site RNA. Our result is in good agreement with the previously reported K_d values for neomycin binding that were obtained by other methods (i.e., SPR studies gave a K_d value of 19 nM) [28, 29], further suggesting that the fluorescein tag does not influence drug binding. The 4-fold difference between our results and those obtained by SPR [28] may reflect possible differences in the experimental conditions (e.g., temperature) or slight influences of the RNA immobilization with biotin or fluorescein tagging. Furthermore, Wong and coworkers demonstrated that higher concentrations of competing ions can decrease the binding of neomycin to the A site RNA to give dissociation constants between 25 and 150 nM [28], consistent with the higher K_d value reported by Wang et al. of 132 nM [29].

Binding of Kanamycin A and Derivatives 2–5 to the A Site Model

Kanamycin A (Figure 3) belongs to the class of 4,6-disubstituted, 2-deoxystreptamine aminoglycosides. Modifications of this drug by *N*-acetylation or *O*-phosphorylation are the two most prevalent mechanisms of clinical resistance [14, 30, 31]. Indeed, the widespread dissemination of the genes for 3′-phosphotransferases among pathogens has been recognized as the clinical cause of the demise of kanamycin therapy [14]. In this study an aminoglycoside 3′-phosphotransferase (APH(3′)-Ia) was employed to convert kanamycin A (**1**) to kanamycin A 3′-phosphate (**2**) [32], and a second bifunctional enzyme, aminoglycoside 2′′-phosphotransferase/aminoglycoside 6′-acetyltransferase (APH(2′′)/AAC(6′)), was used to produce the corresponding singly modified kanamycin A 2′′-phosphate (**3**), doubly modified kanamycin A 6′-acetate 2′′-phosphate (**4**), or kanamycin A 6′-acetate (**5**) (Figure 3) [19].

Kanamycin A has become obsolete in the clinic due the emergence of resistance enzymes that generate aminoglycoside modifications such as those shown in Figure 3 [14]. Thus, understanding the mechanism of resistance and the effects of drug modification on RNA binding is important for the design of more effective antibiotics. To examine whether the kanamycin A-derived compounds could bind to the A site RNA, we carried out titrations with F-AS and compounds **1–5**. For the parent compound, kanamycin A (**1**), the fluorescence signal of F-AS decreased initially upon drug binding until approximately 100 μM, then the fluorescence signal increased and saturation was reached at a higher antibiotic concentration (≥2 mM) (Figure 4A). The two binding events were distinct and well separated, as indicated

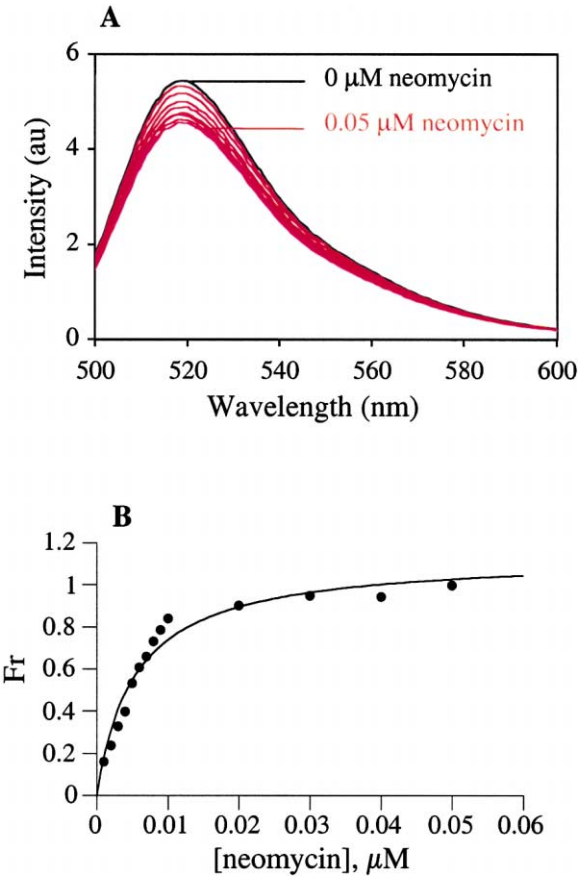

Figure 2. Neomycin Binding to 1 μM F-AS RNA in Buffer A at 37°C

(A) Fluorescence changes associated with neomycin binding to F-AS are shown. Fluorescence emission spectra of 1 μM annealed F-AS before (uppermost curve) and after (lower curves) addition of 0.1–50 nM neomycin. The emission maximum at 519 nm is diminished upon drug binding. The excitation wavelength was 490 nm. The data were collected through 100% saturation.

(B) A representative binding isotherm of the relative fluorescence intensity (Fr) as a function of total neomycin concentration is shown. The solid line represents the fit of the data to Equation 1 (R^2 = 0.958).

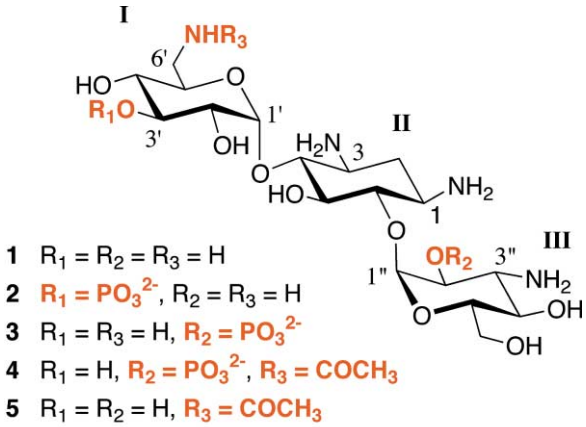

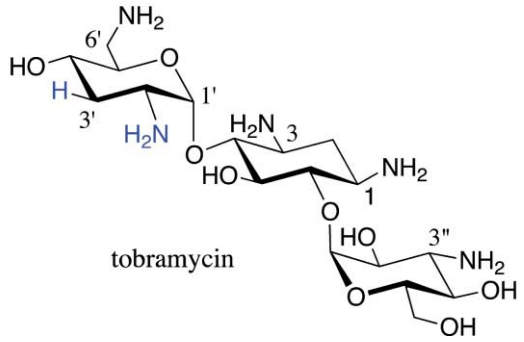

Figure 3. The Subclass of 4,6-Disubstituted Ring II Aminoglycosides

The general structure of kanamycin A (**1**) is shown with functional groups that are modified in red (R_1-R_3). Derivatives **2**–**5** are phosphorylated or acetylated at specific positions (R_1-R_3). The structure of tobramycin is shown for comparison with differences in ring I highlighted in blue.

by the change in fluorescence signal from quenching to enhancement; therefore, each transition was fit independently. Compound **1** exhibited a first binding event with a K_d value of 1.1 ± 0.1 μM and a second binding event with a K_d value of 510 ± 10 μM. The high-affinity event exhibited simple binding behavior (1:1 complex), and the data fit well to Equation 1 (Figure 4B). The low-affinity event was characterized by cooperative behavior, as determined by a non-linear Scatchard plot (our unpublished data) and a Hill plot that gave a non-unity Hill constant, n, of 1.9 (Figure 4C). The high-concentration data fit best to Equation 4 (See Experimental procedures and Figure 4D), which assumes a more complex binding mode (in this case a 2:1 stoichiometry of drug:RNA).

Interestingly, electrospray ionization mass spectrometry studies revealed that the structurally related compound tobramycin displays similar binding behavior to the A site RNA (Figure 3) [33]. Both 1:1 and 2:1 stoichiometries of drug:RNA were observed at low and high tobramycin concentrations, respectively. The first site was attributed to specific interactions mediated by electrostatic, hydrogen bonding, and stacking interactions at the A site bulged residue, whereas the second binding mode was probably governed by nonspecific electrostatic interactions.

As drug binds to RNA and the RNA undergoes a conformational change, the orientation or relative positioning of the 5′ fluorescein tag on the RNA will be altered. Therefore, fluorescence polarization, or anisotropy, can also be used to determine the dissociation constants

Table 1. Dissociation Constants of Aminoglycoside Antibiotics and Kanamycin A Derivatives for the Bacterial A Site RNA

aminoglycoside	K_d (μM)	n[a]
neomycin	0.005 ± 0.002	
1[b]	1.1 ± 0.1	
2	1300 ± 100	2.2
3	2000 ± 100	
4	1700 ± 100	2.3
5	600 ± 20	2.6

[a] Average number of interacting sites.

[b] A second binding event was observed with this compound ($K_{d,2}$ = 510 ± 10 μM; n = 1.9).

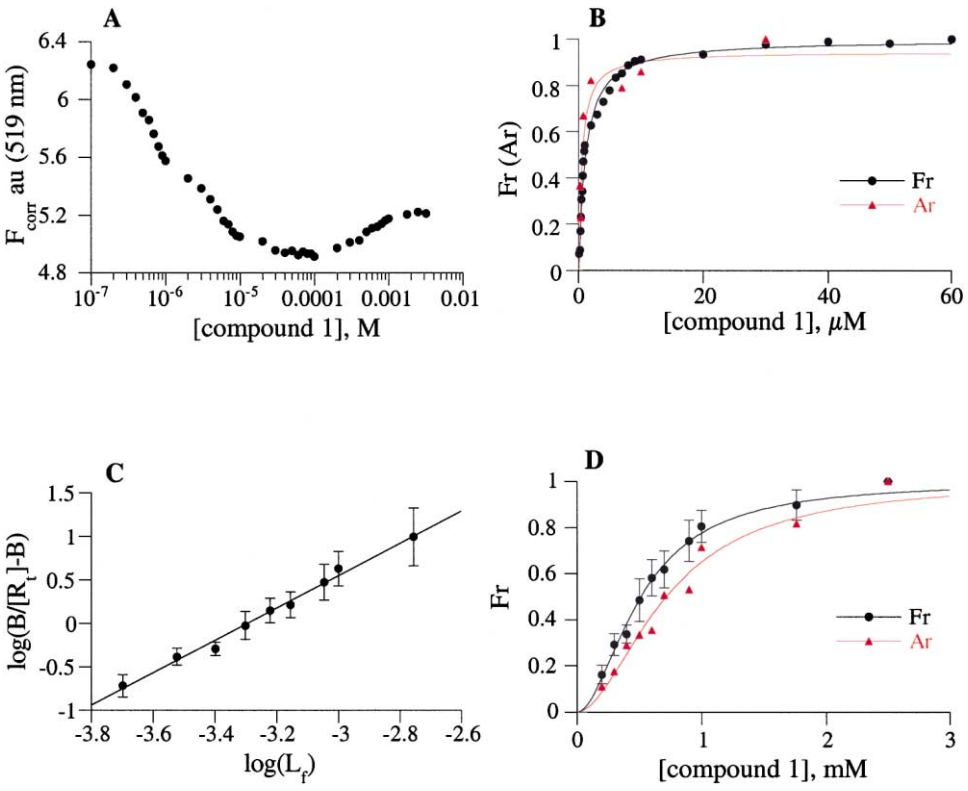

Figure 4. Compound **1** Binding to 1 μM F-AS RNA in Buffer A at 37°C

(A) A plot of the corrected fluorescence at 519 nm as a function of added compound **1** is shown.

(B) A representative binding isotherm of relative fluorescence intensity (Fr) (circles) as a function of total compound **1** concentration (0.1–60 μM) is shown with a fit to Equation 1 ($R^2 = 0.988$). The relative anisotropy (Ar) plot is shown for comparison (triangles) ($R^2 = 0.845$).

(C) A Hill plot for compound **1** at high concentrations (0.2–2.5 mM) was obtained with Equation 3.

(D) Fr (circles) was plotted as a function of total compound **1** concentration (0.2–2.5 mM) and fit to Equation 4 (cooperative binding) ($R^2 = 0.990$). The Ar plot is shown for comparison (triangles) ($R^2 = 0.966$). The error bars in C and D represent the standard deviation from two separate titration experiments.

[34, 35]. Fluorescence anisotropy measurements gave results similar to those of the fluorescence-quenching assay. Fitting the relative anisotropy values (Figures 4B and 4D) for the high- and low-affinity binding modes gave K_d values of 0.5 ± 0.2 μM (1:1 stoichiometry) and 720 ± 33 μM (2:1 stoichiometry), respectively.

Titrations of a fluorescein-tagged human analog (18S) of the 16S A site RNA (sequence 5′-F-GGCGUCG$_{1408}$CUACUUCGGUAA$_{1491}$AAGUCGCC-3′, where F = fluorescein and sequence differences between the 16S and 18S RNAs are underlined) with kanamycin A revealed relatively poor binding ($K_d \approx 100$ μM) (our unpublished data). These results demonstrate the importance of residues such as A1408 and/or G1491 for kanamycin A binding to the A site RNA. In addition, we have examined the influence of ionic strength on the binding of kanamycin A to the A site RNA. Adding higher concentrations of NaCl (up to 1 M) or increasing the pH from 7.4 to 7.8 leads to a 4- to 7-fold reduction of both specific and nonspecific binding (our unpublished data), consistent with previous studies [28].

Titrations of F-AS with kanamycin A derivatives **2–5** led to an increase in fluorescence in every case (Figure 5A). For each derivative examined, no change in fluorescence of F-AS was observed until millimolar concentrations of the drug were added to F-AS. Of the four modified compounds, only **3** exhibited simple binding behavior (i.e., no cooperativity). The binding of derivatives **2**, **4**, and **5** was cooperative, and each displayed a nonlinear Scatchard plot (data not shown) and non-unity Hill constants. The Hill plots are shown in Figure 5B. The Fr-versus-drug-concentration plots in Figure 5C were fit to Equation 1 for derivative **3** or Equation 4 for compounds **2**, **4**, and **5**. The K_d values that were obtained from these fits are reported in Table 1. The changes in binding free energies ($\Delta\Delta G$ values) for compounds **2–5** relative to compound **1** (ΔG_{obs} of **1** − ΔG_{obs} of **2–5**) are −4.3, −4.6, −4.5, and −3.8 kcal/mol, respectively.

The nonlinear Scatchard plots for three (**2**, **4**, and **5**) of the six compounds (and **1** at high concentration) examined in this study were suggestive of cooperative binding modes. In these cases, a Hill-type model was used to obtain the K_d and n values. The non-unity Hill constants for **2**, **4**, and **5**, as well as **1** at high concentration, are not unusual for this class of drugs. Several groups reported that certain 4,6-linked aminoglycosides do not always form 1:1 complexes with the A site RNA construct [28, 33]. Furthermore, the high number of charged groups on these molecules might lead to multiple binding sites on the RNA because of a combination

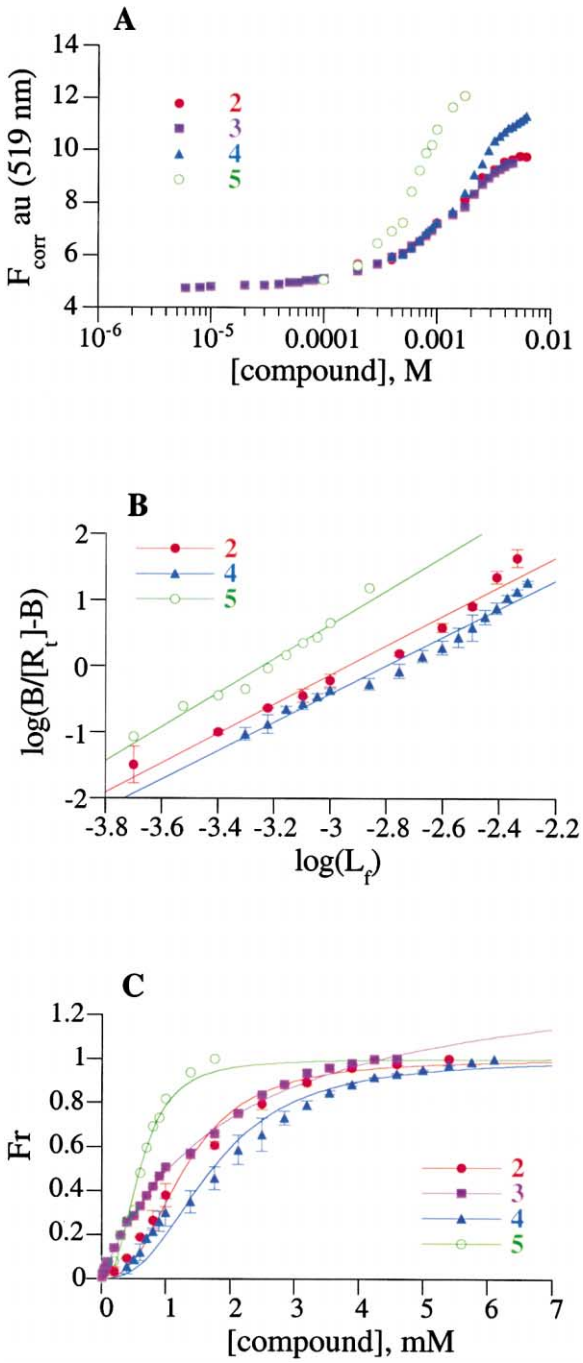

Figure 5. Compounds **2–5** Binding to 1 μM F-AS RNA in Buffer A at 37°C

(A) Plots of the corrected fluorescence at 519 nm as a function of added compound are shown (**2**, closed circles; **3**, squares; **4**, triangles; **5**, open circles).

(B) Hill plots for compounds **2**, **4**, and **5** were obtained with Equation 3.

(C) Plots of Fr as a function of total compound are shown. Data for compounds **2**, **4**, and **5** were fit to Equation 4 (cooperative binding). Data for compound **3** were fit to Equation 1 (1:1 binding). The error bars in B and C represent the standard deviation from two separate titration experiments, except for **5**.

of attractive and repulsive electrostatic interactions. Alternatively, as a result of both RNA and drug flexibility, we may be observing different conformers of drug-RNA complexes. The proposal of such dynamic interactions is not unreasonable given that the target rRNA is a biologically active molecule that takes part in numerous macromolecular binding events.

Previous studies revealed that rings I and II of paromomycin and gentamicin are critical for specific recognition within the A site RNA binding pocket [6, 7, 21, 22]. In the present study, comparisons of binding affinities for the kanamycin derivatives reveals that the presence of specific amino and hydroxyl groups is indeed important for A site RNA recognition. Comparison of neomycin and paromomycin binding to the A site RNA reveals a 10-fold enhancement in binding when a hydroxyl group is replaced by an amino group at the 6′ position of ring I [28, 29]. Phosphorylation of the 3′-hydroxyl group of ring I on kanamycin A has a much more dramatic effect on its binding to the A site RNA. An identical group (OH) on paromomycin's 3′ position makes backbone contacts in the paromomycin-RNA complex [6, 7, 22]. Thus, it is not surprising that a >1000-fold-diminished binding affinity for F-AS is observed when **1** is converted to **2**.

Ring III of the 4,6-linked kanamycin A likely makes important contributions to the binding affinity, although the contacts will be different from ring III of the 4,5-linked compounds neomycin and paromomycin because of different positioning (see Figures 1 and 3 for a comparison of the structures). The apparent dissociation constant of neamine, which comprises rings I and II of neomycin (Figure 1B), with A site RNA constructs is between 10 and 24 μM [36, 37], compared to a K_d of 1.1 μM for kanamycin A. Ring III of gentamicin, which is structurally similar to kanamycin A, makes additional sequence-specific contacts with the A site RNA when it is compared to paromomycin [6, 7]. Specifically, the 2′′ hydroxyl group on gentamicin, which is also found on kanamycin A, is within hydrogen bonding distance of G1405 (O6) and U1406 (O4) [7]. Thus, 2000- and 1700-fold-diminished binding affinities for 2′′-phosphorylated derivatives **3** and **4**, respectively, are consistent with a disruption of these important RNA-ligand contacts and are probably due to electrostatic repulsions between the derivatives and the RNA backbone. Similarly, disruption of the hydrogen bonding contacts between the 6′-amino group and the A site RNA will be severely compromised upon acetylation at this site (derivatives **4** and **5**). As reported in Table 1, derivative **5** shows a 600-fold-diminished binding affinity compared to that of **1**. Taken together, our results suggest that modification of functional groups that most likely contact A site residues will lead to a loss of the specific binding mode observed at low concentrations of kanamycin A, whereas nonspecific binding modes with one or more sites of interaction will dominate for derivatives **2–5**.

Computer Modeling

Figure 6 shows the energy-minimized structure of kanamycin A (**1**) bound in the A site of rRNA template. This compound occupies the pocket that is formed by A1492

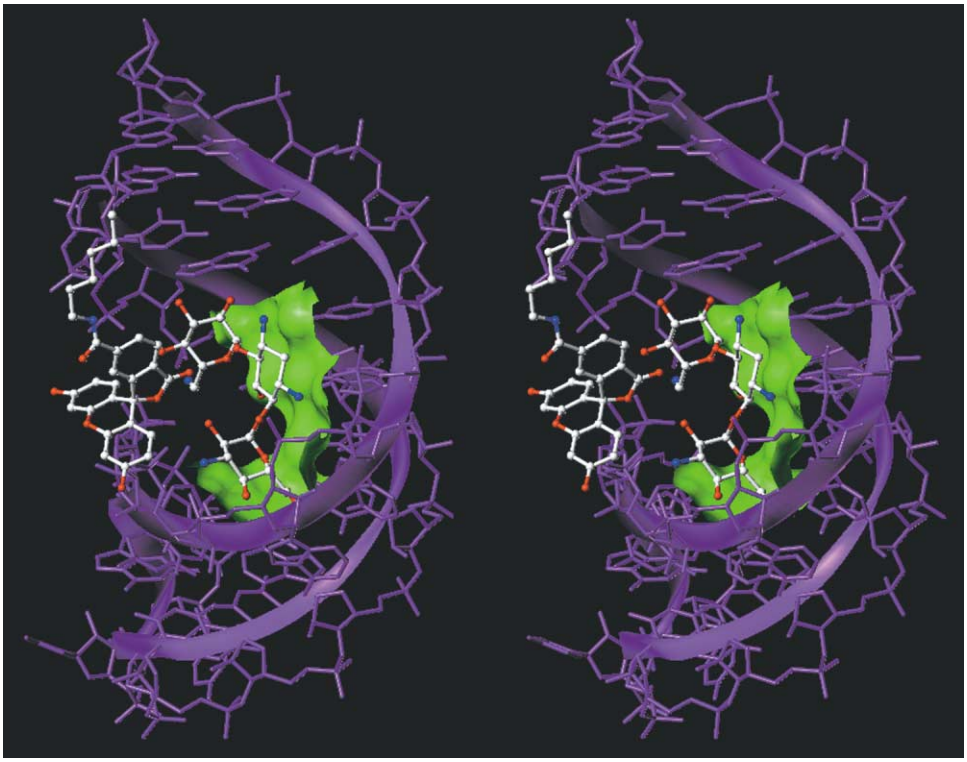

Figure 6. Stereo View of the Computational Model for the Complex between the A Site RNA Template and Kanamycin A

The lowest-energy conformation of the fluorescein tag is shown in ball-and-stick representation, and a portion of the binding site for kanamycin A (color-coded ball-and-stick representation: C, white; N, blue; O, red) is shown as a green Connolly surface on the A site RNA (violet capped-stick representation).

and the A1408•A1493 motif, as was observed with paromomycin and gentamicin [6, 7]. In the uncomplexed RNA, the fluorescein tag does not contact the RNA and points toward the solution with free rotation. After the drug is bound, the region spanning the binding site for kanamycin A was accessible to various conformations of the fluorescein tag appended at the 5′ terminus. In the analysis of 1,132 conformations of the fluorescein tag with kanamycin A present, approximately 50% of the conformations that were closer to the kanamycin binding site showed lower energy than the remainder. The lowest-energy conformation brings the fluorescein tag close to the kanamycin A binding site and, in fact, an overlay of all the conformations shows that the best low-energy conformations capped the binding site of kanamycin A on the A site RNA template. This observation indicates the likelihood of direct interactions between the aminoglycoside ligand bound in the A site of the RNA template and the fluorescein tag at the 5′ terminus following drug binding, suggesting a mechanism for the observed changes in fluorescence intensity of the attached dye molecule. Differences in fluorescence intensities between the aminoglycoside-F-AS complexes reflect variations in the drug binding modes. The fluorescence quenching or enhancement mechanism probably depends on the manner in which the dye molecule interacts near the surface of the drug binding site, which will vary with aminoglycoside antibiotic structure and binding orientation.

Anisotropy experiments are also consistent with the modeling studies in which the fluorescein becomes situated closer to the RNA surface in the presence of antibiotics. As kanamycin A binds to F-AS, fluorescence anisotropy increases (the anisotropy value, r, is 0.045 in the absence of drug and 0.076 at 2.5 mM kanamycin A), indicating that the movement of the fluorescein tag is more constrained in the drug-RNA complex. Fitting of the relative anisotropy values for the high- and low-affinity binding modes is shown in Figures 4B and 4D.

Antibiotic Activities of Modified Aminoglycosides

The minimum inhibitory concentration (MIC) of kanamycin A is 4 μg/ml for *E. coli* JM109, but is elevated by >500-fold (2048 μg/ml) in *E. coli* JM109(pSF815A), which expresses the bifunctional enzyme APH(2″)/AAC(6′) [19]. Similarly, the MIC levels are elevated 250-fold in *E. coli* strains that express the aminoglycoside 3′-phosphotransferases APH(3′)-Ia and APH(3′)-IIa (S. Vakulenko and S.M., unpublished data). Thus, a loss in antibacterial activities associated with these modified aminoglycoside antibiotics is consistent with a loss in their RNA binding abilities. One possible reason for the more dramatic loss in RNA binding upon modification (1000- to 2000-fold reduction in binding) as compared to smaller differences in MIC values (250- to 512-fold) is that the in vitro experiments were conducted with fully modified compounds, whereas the compounds are likely not to be 100% modified in the cellular environ-

ment [19]. Furthermore, MIC is a more complex expression of interactions of the drug with living bacteria, and its direct comparison to dissociation constants of aminoglycosides with the A site RNA should be made with caution. Nonetheless, a clear trend is observed between the reduced RNA binding abilities of the modified antibiotics and their attenuated antimicrobial activity in vivo.

Conclusions

The fluorescein-tagged 27 nucleotide RNA (F-AS) used in this study was the same sequence of RNA that was used previously for NMR and chemical probing [6–13], mass-spectrometric [38], and surface plasmon resonance (SPR) [28] studies; therefore, direct comparisons can be made between the results described here and results for other aminoglycosides described elsewhere. In the case of SPR studies, the 27 nucleotide RNA was tagged with biotin at the 5′ end, which had no apparent influence on the binding of aminoglycosides [28]. In our studies a 6 carbon linker attached to fluorescein resides at the same location on the 5′ terminus. The fluorescein tag is within 15 Å of linear distance to the aminoglycoside binding site, with little restriction on its motion. The low anisotropy of fluorescein is indicative of a high rotational freedom, as was demonstrated previously with 5-carboxyfluorescein-tagged RNA [39]. Upon drug-induced RNA bending, however, the tag becomes positioned closer to the binding site, as determined by computer modeling and simulations, and has less rotational freedom. These changes in the fluorescein position lead to subsequent changes in the fluorescence intensity (vide infra).

The present report describes the ability of the fluorescein-tagged A site RNA of the bacterial ribosome to bind modified aminoglycosides. The utility of the system described herein for quantitative screening of antibiotics has been demonstrated for several aminoglycoside antibiotics that are known to bind to the A site of the ribosome. Furthermore, we have shown for the first time in a quantitative manner that modified aminoglycosides, the products of the reactions catalyzed by the resistance enzymes, suffer from attenuated binding ability to the A site of 16S rRNA, which correlates well with the loss of antibacterial ability in resistant organisms that harbor these enzymes. Major efforts are currently underway in a number of laboratories to develop antibiotics that avoid the resistance mechanisms [36, 40–44]. A key to success in these endeavors will be the identification of validated targets for antibiotics and the ability to assess ligand binding to the site in a convenient and rapid manner. Thus, future efforts in this area will include the development of more sensitive fluorophores within the RNA to detect drug binding and immobilization of target RNAs for multiple rounds of screening.

Significance

The high toxicity and emergence of antibiotic resistance has limited the usefulness of the aminoglycoside class of antibacterials. One prevalent mechanism of resistance involves enzymatic phosphorylation or acetylation of specific functional groups on the aminoglycosides. The goal of this work was to test the hypothesis that such modifications of aminoglycoside functional groups by natural resistance enzymes will cause these antibiotics to have unfavorable interactions with their natural biological target, the bacterial A site from 16S rRNA, because of unfavorable electrostatic or van der Waals interactions. We have isolated four kanamycin A derivatives that are the products of natural resistance enzymes and quantitatively demonstrated that they do in fact have reduced affinity for the bacterial ribosomal A site RNA. The 600- to 2000-fold reduction in binding affinities of the phosphorylated or acetylated aminoglycosides correlates well with their diminished antibacterial activities. These results demonstrate that the natural resistance enzymes modify specific functional groups on the aminoglycoside antibiotics that are critical for making contacts with the target RNA.

Experimental Procedures

General

Neomycin sulfate (≥85% neomycin B, ≤15% neomycin C) and kanamycin sulfate (kanamycin A, <5% kanamycin B) were purchased from Sigma (St. Louis, Missouri).

Isolation of Turnover Products of Kanamycin A

Compounds **2–5** were prepared by slight modifications of literature procedures [19, 32]. *E. coli* JM109(pSF815A) or JM83(pTZ18u) was grown in 6 liters of Terrific Broth up to the late logarithmic phase, then cells were harvested by centrifugation. The cell pellet (32 g wet cell paste) was resuspended in 100 ml buffer (50 mM HEPES [pH 7.5], supplemented with 0.2 mM dithiothreitol, and 1 mM phenylmethylsulfonyl fluoride), lysed by ultrasonication, and centrifuged. The resulting supernatant was treated with 1 g streptomycin sulfate and centrifuged at 80,000 *g* for 1 hr. For the removal of small molecules (such as ATP and coenzyme A), the supernatant was dialyzed against 10 mM HEPES (pH 7.5) supplemented with 1 mM dithiothreitol.

The large-scale aminoglycoside phosphorylation procedure for production of **2** or **3** was according to a modification of the method of Siregar et al. [32]. The phosphorylation reaction mixture consisted of the appropriate dialysate, 11 mM magnesium chloride, 22 mM potassium chloride, and 200 mM HEPES at pH 7.5 in a total volume of 250 ml. The reaction was started by the addition of 100 mg kanamycin A, 40.6 mg phosphoenol pyruvate, 31.5 units of pyruvate kinase, and 0.51 g ATP, and the mixture was incubated at 37°C for 12 hr. Subsequently, the reaction mixture was put in a boiling water bath for 10 min. The mixture was centrifuged at 3200 *g* for 15 min. The supernatant was concentrated in vacuo, then was lyophilized. The residue was taken up in 200 ml methanol and centrifuged (3200 *g* for 15 min). The precipitate was washed with methanol and was suspended in a mixture of 10 ml water, 10 ml ethyl acetate, and 10 ml methanol, then centrifuged at 3200 *g* for 15 min. This step was repeated once. The collected pellet was resuspended in 15 ml water, and the insoluble materials were discarded after centrifugation (3200 *g* for 15 min). The supernatant was loaded onto a CG-50 column (NH_4^+ salt, 20 cm × 1 cm). The column was washed with 500 ml water, followed by elution with a linear gradient of NH_4OH (0 to 2%, 500 ml) in water. Fractions that gave positive results with the ninhydrin test were pooled and concentrated in vacuo to dryness. The phosphorylated kanamycin A was pure, as determined by spectroscopic characterizations that matched previous results.

For acetylation of kanamycin A to produce **5**, the reaction was set up for a biphasic acetyl coenzyme A recycling method, as described by Ouyang and coworkers [45]. Kanamycin A (100 mg) was dissolved in 200 mM HEPES buffer (pH 7.5), supplemented with 1 mM dithiothreitol in a total volume of 50 ml. A 4 mg portion of coenzyme A was dissolved in the kanamycin A solution. A 2 mg

portion of 4-dimethylaminopyridine (DMAP) was dissolved in 5 ml toluene, and the two solutions were combined to form two phases, which were stirred. A 0.5 ml portion of the enzyme dialysate, prepared as described above, was added to the aqueous layer, and the mixture was gently stirred at 37°C. Finally, acetic anhydride (250 μl) was added very slowly into the organic layer. Additional portions of kanamycin A (100 mg), and enzyme dialysate (1 ml) were added at 2 and 4 hr of the reaction. The reaction was then stopped after 6 hr by boiling the solution in a water bath for 10 min. The reaction product was isolated as described for the phosphorylated product. All reactions were monitored by tlc (EtOH:MeOH:HOAc:H_2O, 5:5:4.5:4.5).

Preparation of F-AS RNA

A 5′-fluorescein-labeled A site model, F-AS (5′-F-GGCGUCACAC CUUCGGGUGAAGUCGCC-3′), was synthesized by via standard silyl phosphoramidite chemistry with reagents from Glen Research (Sterling, Virginia). The human analog RNA (5′-F-GGCGUCGCUA CUUCGGUAAAAGUCGCC-3′) was obtained from Dharmacon Research (Lafayette, Colorado). The RNAs were purified by electrophoresis on denaturing (8 M urea) 15% polyacrylamide gels, followed by electroelution with 1× TBE (90 mM Tris-HCl, 90 mM boric acid, and 2.5 mM Na_2EDTA [pH 8.3]) in an Amicon centrilutor and Centricon 3 units (Amicon). The F-AS RNA and human analog RNA were stored at −20°C in 10 mM HEPES (pH 7.4). RNA concentrations were determined spectrophotometrically with molar extinction coefficients of 253,300 $M^{-1}\cdot cm^{-1}$ and 258,100 $M^{-1}\cdot cm^{-1}$ for F-AS and the human analog, respectively. For renaturing, the RNAs (~150 μM) were placed in a water bath at 20°C, heated to 85°C for 1 min, then slowly cooled back to 20°C over a 2 hr period.

Fluorescence Measurements

Fluorescence experiments were performed on a Spex Fluoromax luminescence spectrometer. The RNA solutions were prepared as 1 μM F-AS in buffer A (10 mM HEPES [pH 7.4], 150 mM NaCl, and 3 mM Na_2EDTA). Fluorescence emission spectra were obtained with an excitation wavelength of 490 nm, with a band pass of 2.9 nm (0.7 mm slit width) over the range of λ_{em} = 500–600 nm. All measurements were taken at 37°C. Samples were incubated in a temperature-controlled cuvette holder in the Fluoromax for 2 min before fluorescence intensities were measured. Aliquots of the antibiotic were added sequentially, and 2 min of equilibration time were allowed before each fluorescence measurement.

Fluorescence intensities were corrected for volume changes according to the following equation: $F_{i,corr} = F_{i,obs} \times V_i/V_0$, where $F_{i,corr}$ is the corrected intensity for point i of the titration, $F_{i,obs}$ is the measured intensity at point i, V_i is the volume after the i^{th} addition, and V_0 is the initial volume (typically 350 μl).

Determination of K_d Values

The K_d values for simple binding were determined by plotting Fr against the total ligand concentration, $[L_t]$, where Fr is the fraction of fluorescence intensity due to the bound species. $Fr = (F_{0,corr} - F_{i,corr})/(F_{0,corr} - F_{F,corr})$, where $F_{0,corr}$, $F_{i,corr}$, and $F_{F,corr}$ are values of the sample at the initial point (all free), the sample at point i in the titration, or the sample at the final titration point (all bound), respectively. The data were fit to the expression described by Equation 1, where $[R_t]$ is the total RNA concentration and c is a constant that relates fluorescence intensity to concentration (typical values are in the range of 10^9 M^{-1}). The value of $[R_t]$ was 1 μM.

$$Fr = ((K_d + [L_t] + [R_t]) - ((K_d + [L_t] + [R_t])^2 - 4[L_t][R_t])^{0.5})/2c \quad (1)$$

Scatchard plots [46] (Equation 2) were used to determine whether binding was simple or cooperative (B is the bound drug-RNA complex concentration, and $[L_f]$ is the free ligand concentration).

$$B/[L_f] = -B/K_d + [R_t]/K_d \quad (2)$$

Binding modes were described as cooperative if the nonlinear Scatchard plot was concave down. Hill plots [46] (Equation 3) were used to determine the value of n, which represents the average number of interacting sites.

$$\log (B/([R_t] - B)) = n(\log [L_f]) - \log K_d \quad (3)$$

The Hill constant n was also used to determine K_d with Equation 4.

$$Fr = [L_t]^n/([L_t]^n + K_d^n) \quad (4)$$

Fluorescence Anisotropy Measurements

Fluorescence anisotropy (r) was determined from Equation 5, in which I is the measured fluorescence intensity with polarizers vertically (v) or horizontally (h) oriented. The first letter refers to the excitation polarizer, and the second refers to the emission polarizer. The grating factor, G, is defined by the ratio I_{hv}/I_{hh} [34, 35].

$$r = (I_{vv} - GI_{vh})/(I_{vv} + 2GI_{vh}) \quad (5)$$

The K_d values were determined by plotting Ar (relative anisotropy) against the total ligand concentration, $[L_t]$, where Ar is the fraction of r due to the bound species. $Ar = (r_{0,corr} - r_{i,corr})/(r_{0,corr} - r_{F,corr})$, where $r_{0,corr}$, $r_{i,corr}$, and $r_{F,corr}$ are the r values at the initial point (all free), at point i in the titration, or at the final titration point (all bound), respectively.

Molecular Modeling

The NMR structure of the A site RNA-paromomycin complex [6] was obtained from the Research Collaboratory for Structural Bioinformatics Protein Data Bank, and paromomycin was replaced with kanamycin A (1). First, the common rings I and II in paromomycin, and kanamycin A were retained in their NMR conformations, and the remainder of the structure was adjusted to that of kanamycin A. The negative charges on the A site RNA-paromomycin complex were neutralized by the addition of 22 Na^+ ions by the use of "addIons" utility in Amber 5.0 suite of programs [47, 48]. The entire complex was solvated in a rectangular box of TIP3 waters (10 Å thickness) and was energy minimized for 10,000 iterations with the Amber 5.0 package. The coordinates of the complex were extracted, and the fluorescein tag was built at the 5′ end of the A site template, linking it to guanosine. The 5′-fluorescein tag was energy minimized with the Tripos force field with Gasteiger charges, as implemented in Sybyl [49]. A systematic search was performed with all the torsions in the linker between the 5′-terminal guanosine and the fluorescein tag, C4′-C5′ and C5′-O5′ torsions on the 5′-guanosine (a total of 10 torsion angles). The increment for each torsion angle was 60°, and energies of all the conformations were evaluated. A set of 1,132 conformations that satisfied the van der Waals criterion were kept, and 105,988 conformations that did not satisfy this criterion in the search process were rejected. The energies of 1,132 conformations were analyzed with respect to the conformation of the fluorescein tag.

Acknowledgments

This work was supported by a National Institutes of Health grant to C.S.C. We thank Leonard Lamsen for technical assistance.

Received: August 21, 2001
Revised: January 24, 2002
Accepted: January 25, 2002

References

1. Gale, E.F., Cundliffe, E., Reynolds, P.E., Richmond, M.H., and Waring, M.J. (1972). The Molecular Basis of Antibiotic Action (New York: John Wiley & Sons).
2. Moazed, D., and Noller, H.F. (1987). Interaction of antibiotics with functional sites in 16S ribosomal RNA. Nature *327*, 389–394.
3. Woodcock, J., Moazed, D., Cannon, M., Davies, J., and Noller, H.F. (1991). Interaction of antibiotics with A- and P-site-specific bases in 16S ribosomal RNA. EMBO J. *10*, 3099–3103.
4. Purohit, P., and Stern, S. (1994). Interactions of a small RNA with antibiotic and RNA ligands of the 30S subunit. Nature *370*, 659–662.
5. Botto, R.E., and Coxon, B. (1983). Nitrogen-15 nuclear magnetic resonance spectroscopy of neomycin B and related aminoglycosides. J. Am. Chem. Soc. *105*, 1021–1028.
6. Fourmy, D., Recht, M.I., Blanchard, S.C., and Puglisi, J.D. (1996).

Structure of the A site of *Escherichia coli* 16S ribosomal RNA complexed with an aminoglycoside antibiotic. Science *274*, 1367–1371.

7. Yoshizawa, S., Fourmy, D., and Puglisi, J.D. (1998). Structural origins of gentamicin antibiotic action. EMBO J. *17*, 6437–6448.
8. Hermann, T., and Westhof, E. (1999). Docking of cationic antibiotics to negatively charged pockets in RNA folds. J. Med. Chem. *42*, 1250–1261.
9. Miyaguchi, H., Narita, H., Sakamoto, K., and Yokoyama, S. (1996). An antibiotic-binding motif of an RNA fragment derived from the A-site-related region of *Escherichia coli* 16S rRNA. Nucleic Acids Res. *24*, 3700–3706.
10. Recht, M.I., Fourmy, D., Blanchard, S.C., Dahlquist, K.D., and Puglisi, J.D. (1996). RNA sequence determinants for aminoglycoside binding to an A-site rRNA model oligonucleotide. J. Mol. Biol. *262*, 421–436.
11. Blanchard, S.C., Fourmy, D., Eason, R.G., and Puglisi, J.D. (1998). rRNA chemical groups required for aminoglycoside binding. Biochemistry *37*, 7716–7724.
12. Fourmy, D., Yoshizawa, S., and Puglisi, J.D. (1998). Paromomycin binding induces a local conformational change in the A-site of 16 S rRNA. J. Mol. Biol. *277*, 333–345.
13. Recht, M.I., Douthwaite, S., Dahlquist, K.D., and Puglisi, J.D. (1999). Effect of mutations in the A site of 16 S rRNA on aminoglycoside antibiotic-ribosome interaction. J. Mol. Biol. *286*, 33–43.
14. Wright, G.D., Berghuis, A.M., and Mobashery, S. (1998). Aminoglycoside antibiotics: structures, functions and resistance. In Resolving the Antibiotic Paradox: Progress in Understanding Drug Resistance and Development of New Antibiotics, B.P. Rosen and S. Mobashery, eds. (New York: Plenum Press), pp. 27–69.
15. Davies, J. (1994). Inactivation of antibiotics and the dissemination of resistance genes. Science *264*, 375–382.
16. Davies, J., and Webb, V. (1998). Antibiotic resistance in bacteria. In Emerging Infections, R.M. Krause, ed. (New York: Academic Press), pp. 239–273.
17. Wright, G.D. (1999). Aminoglycoside-modifying enzymes. Curr. Opin. Microbiol. *2*, 499–503.
18. Kotra, L.P., Golemi, D., Vakulenko, S., and Mobashery, S. (2000). Bacteria fight back. Chemistry & Industry *10*, 341–344.
19. Azucena, E., Grapsas, I., and Mobashery, S. (1997). Properties of a bifunctional bacterial antibiotic resistance enzyme that catalyzes ATP-dependent 2′′-phosphorylation and acetyl-CoA-dependent 6′-acetylation of aminoglycosides. J. Am. Chem. Soc. *119*, 2317–2318.
20. Daigle, D.M., Hughes, D.W., and Wright, G.D. (1999). Prodigious substrate specificity of AAC(6′)-APH(2′′), an aminoglycoside antibiotic resistance determinant in enterococci and staphylococci. Chem. Biol. *6*, 99–110.
21. Carter, A.P., Clemons, W.M., Broderson, D.E., Morgan-Warren, R.J., Wimberly, B.T., and Ramakrishnan, V. (2000). Functional insights from the structure of the 30S ribosomal subunit and its interactions with antibiotics. Nature *407*, 340–348.
22. Vicens, Q., and Westhof, E. (2001). Crystal structure of paromomycin docked into the eubacterial ribosomal decoding A site. Structure *9*, 647–658.
23. Llano-Sotelo, B., and Chow, C.S. (1999). RNA-aminoglycoside antibiotic interactions: fluorescence detection of binding and conformational change. Bioorg. Med. Chem. Lett. *9*, 213–216.
24. Fang, X., Pan, T., and Sosnick, T.R. (1999). A thermodynamic framework and cooperativity in the tertiary folding of a Mg^{2+}-dependent ribozyme. Biochemistry *38*, 16840–16846.
25. Jhaveri, S.D., Kirby, R., Conrad, R., Maglott, E.J., Bowser, M., Kennedy, R.T., Glick, G., and Ellington, A.D. (2000). Designed signaling aptamers that transduce molecular recognition to changes in fluorescence intensity. J. Am. Chem. Soc. *122*, 2469–2473.
26. Stojanovic, M.N., de Prada, P., and Landry, D.W. (2001). Aptamer-based folding fluorescent sensor for cocaine. J. Am. Chem. Soc. *123*, 4928–4931.
27. Lynch, D.C., and Schimmel, P.R. (1974). Cooperative binding of magnesium to transfer ribonucleic acid studied by a fluorescent probe. Biochemistry *13*, 1841–1852.
28. Wong, C.-H., Hendrix, M., Priestley, E.S., and Greenberg, W.A. (1998). Specificity of aminoglycoside antibiotics for the A-site of the decoding region of ribosomal RNA. Chem. Biol. *5*, 397–406.
29. Wang, Y., Hamasaki, K., and Rando, R.R. (1997). Specificity of aminoglycoside binding to RNA constructs derived from the 16S rRNA decoding region and the HIV-RRE activator region. Biochemistry *36*, 768–779.
30. Shaw, K.J., Rather, P.N., Hare, R.S., and Miller, G.H. (1993). Molecular genetics of aminoglycoside resistance genes and familial relationships of the aminoglycoside-modifying enzymes. Microbiol. Rev. *57*, 138–163.
31. Miller, G.H., Sabatelli, F.J., Hare, R.S., Glupczynski, Y., Mackey, P., Shlaes, D., Shimizu, K., and Shaw, K.J. (1997). The most frequent aminoglycoside resistance mechanisms—changes with time and geographic area: a reflection of aminoglycoside usage patterns. Clin. Infect. Dis. *24*, S46–S62.
32. Siregar, J.J., Miroshnikov, K., and Mobashery, S. (1995). Purification, characterization, and investigation of the mechanism of aminoglycoside 3′-phosphotransferase type Ia. Biochemistry *34*, 12681–12688.
33. Sannes-Lowery, K.A., Griffey, R.H., and Hofstadler, S.A. (2000). Measuring dissociation constants of RNA and aminoglycoside antibiotics by electrospray ionization mass spectrometry. Anal. Biochem. *280*, 264–271.
34. Chen, R.F., and Bowman, R.L. (1965). Fluorescence polarization: measurement with ultraviolet-polarizing filters in a spectrophotofluorometer. Science *147*, 729–732.
35. Lackowicz, J.R. (1983). Principals of Fluorescence Spectroscopy. (New York: Plenum Press).
36. Sucheck, S.J., Wong, A.L., Koeller, K.M., Boehr, D.D., Draker, K.-A., Sears, P., Wright, G.D., and Wong, C.-H. (2000). Design of bifunctional antibiotics that target bacterial rRNA and inhibit resistance-causing enzymes. J. Am. Chem. Soc. *122*, 5230–5231.
37. Ding, Y., Hofstadler, S.A., Swayze, E.E., and Griffey, R.H. (2001). An efficient synthesis of mimetics of neamine for RNA recognition. Org. Lett. *3*, 1621–1623.
38. Griffey, R.H., Hofstadler, S.A., Sannes-Lowery, K.A., Ecker, D.J., and Crooke, S.T. (1999). Determinants of aminoglycoside-binding specificity for rRNA by using mass spectrometry. Proc. Natl. Acad. Sci. USA *96*, 10129–10133.
39. Tuschl, T., Gohlke, C., Jovin, T.M., Westhof, E., and Eckstein, F. (1994). A three-dimensional model for the hammerhead ribozyme based on fluorescence measurements. Science *266*, 785–789.
40. Haddad, J., Vakulenko, S., and Mobashery, S. (1999). An antibiotic cloaked by its own resistance enzyme. J. Am. Chem. Soc. *121*, 11922–11923.
41. Roestamadji, J., Grapsas, I., and Mobashery, S. (1995). Mechanism-based inactivation of bacterial aminoglycoside 3′-phosphotransferases. J. Am. Chem. Soc. *117*, 80–84.
42. Michael, K., and Tor, Y. (1998). Designing novel RNA binders. Chem. Eur. J. *4*, 2091–2098.
43. Nunns, C.L., Spence, L.A., Slater, M.J., and Berrisford, D.J. (1999). Synthesis of neamine libraries for RNA recognition using solution phase chemistry. Tetrahedron Lett. *40*, 9341–9345.
44. Ding, Y., Swayze, E.E., Hofstadler, S.A., and Griffey, R.H. (2000). Efficient synthesis of neomycin B related aminoglycosides. Tetrahedron Lett. *41*, 4049–4052.
45. Ouyang, T., Walt, D.R., and Patel, S.S. (1990). Enzyme-catalyzed synthesis of citric acid using acetyl-coenzyme A recycling in a 2-phase system. Bioorg. Chem. *18*, 131–135.
46. Connors, K.A. (1987). Binding Constants, The Measurement of Molecular Complex Stability. (New York: John Wiley & Sons).
47. Case, D.A., Pearlman, D.A., Caldwell, J.W., Cheatham, T.E., III, Ross, W.S., Simmerling, C.L., Darden, T.A., Merz, K.M., Stanton, R.V., Cheng, A.L., et al. (1997) AMBER *5*. (San Francisco, CA: University of California).
48. Pearlman, D.A., Case, D.A., Caldwell, J.W., Ross, W.S., Cheatham, T.E., III, DeBolt, S., Ferguson, D.M., Seibel, G.L., and Kollman, P.A. (1995). Amber 5. Comp. Phys. Commun. *91*, 1–41.
49. Tripos Associates. (1998). Sybyl version 6.5. (St. Louis, MO).